PAPER

Thermal conductivity and structural behavior of confined H_2 from molecular dynamics simulation

IOP Publishing Nanotechnology
Nanotechnology 35 (2024) 215403 (8pp) https://doi.org/10.1088/1361-6528/ad2814

Thermal conductivity and structural behavior of confined H_2 from molecular dynamics simulation

Farrokh Yousefi[1,2], **Omid Farzadian**[3] and **Mehdi Shafiee**[1,2]

[1] Department of Electrical and Computer Engineering, Nazarbayev University, Astana 010000, Kazakhstan
[2] Energetic Cosmos Laboratory, Nazarbayev University, Astana 010000, Kazakhstan
[3] Department of Physics, School of Sciences and Humanities, Nazarbayev University, Astana 010000, Kazakhstan

E-mail: mehdi.shafiee@nu.edu.kz

Received 13 November 2023, revised 19 January 2024
Accepted for publication 9 February 2024
Published 8 March 2024

Abstract

In this work, we perform equilibrium molecular dynamics simulation to study the thermal conductivity of hydrogen molecules (H_2) under extreme confinement within graphene nanochannel. We analyze the structural behavior of H_2 molecules inside the nanochannel and also examine the effect of nanochannel height, the number of H_2 molecules, and temperature of the system on the thermal conductivity. Our results reveal that H_2 molecules exhibit a strong propensity for absorption onto the nanochannel wall, consequently forming a dense packed layer in close to the wall. This phenomenon significantly impacts the thermal conductivity of the confined system. We made a significant discovery, revealing a strong correlation between the mass density near the nanochannel wall and the thermal conductivity. This finding highlights the crucial role played by the density near the wall in determining the thermal conductivity behavior. Surprisingly, the average thermal conductivity for nanochannels with a height (h) less than 27 Å exhibited an astonishing increase of over 12 times when compared to the bulk. Moreover, we observe that increasing the nanochannel height, while the number of H_2 molecules fixed, leads to a notable decrease in thermal conductivity. Furthermore, we investigate the influence of temperature on thermal conductivity. Our simulations demonstrate that higher temperature enhance the thermal conductivity due to increased phonon activity and energy states, facilitating more efficient heat transfer and higher thermal conductivity. To gain deeper insights into the factors affecting thermal conductivity, we explored the phonon density of states. Studying the behavior of hydrogen in confined environments can offer valuable insights into its transport properties and its potential for industrial applications.

Keywords: hydrogen confinement, graphene nanochannel, thermal conductivity, molecular dynamics, density profile, Green–Kubo method

Introduction

Nanoconfined systems exhibit exceptional properties that have garnered significant interest in the field of nanotechnology. The unique behavior and characteristics observed when materials are confined at the nanoscale open up exciting possibilities for technological advancements. In recent years, for example, huge simulations were performed for water confinement and obtained thermal conductivity [1, 2], dielectric [3, 4], permittivity and ferroelectricity [5], and optoelectronic properties [6]. For example, when considering the in-plane dielectric constant of nano-confined water with a height of 6.5 Å, it is observed to be twice that of bulk water. Moreover, Joseph *et al* [7] studied transport properties of confined water in carbon nanotube. They results show that the structure of water, including the orientations of OH bonds and hydrogen bonding, directly impacts the enhancement of flow rates in the depletion region where water concentration is less than 5% of the bulk value.

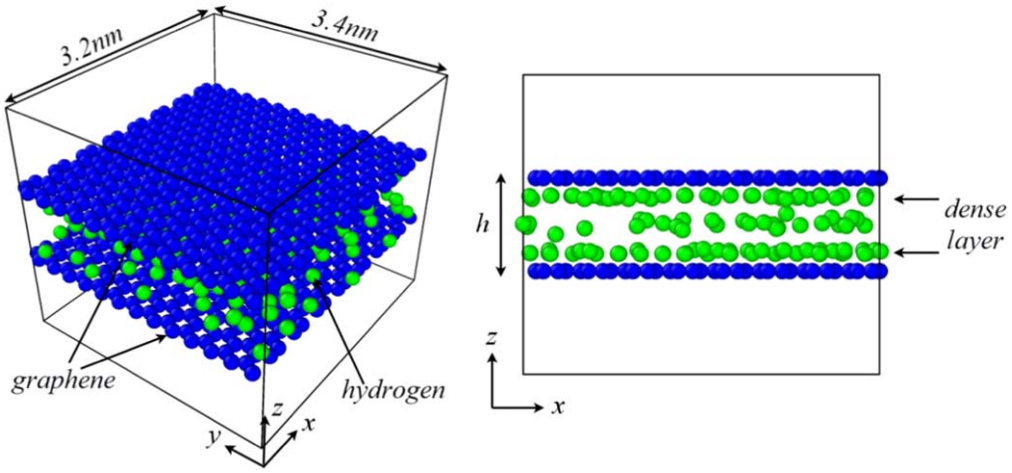

Figure 1. Illustration of the simulation setup. The upper and lower sheets are the rigid graphene and green-colored particles are the H_2 molecules.

Furthermore, Ghosh *et al* [8], conducted a study on the structural behavior of supercritical Lennard-Jones fluids when confined. Their research revealed the presence of the Frenkel line within the supercritical regime using molecular dynamics simulations. Additionally, their findings demonstrated that argon gas exhibits a layered pattern at high pressures within nanochannels. Jabbari *et al* [9], have authored a comprehensive review paper on thermal conductivity and viscosity of nano-fluids, serving as an excellent and reliable reference for readers seeking in-depth insights into this subject.

Also, hydrogen is another simple molecule that has a diverse range of industrial applications and has gained momentum as a possible fuel [10–16]. However, at ambient conditions, hydrogen exhibits a relatively low volumetric energy density. To solve the problem, one way is compressing the hydrogen up to 100 MPa using electrochemical hydrogen compression (EHC) [17, 18]. Another promising approach to enhance the density of hydrogen involves its confinement within nanochannels, leveraging the expansive surface area provided by these structures. By confining hydrogen within nanoscale nanochannels, the available surface area is maximized, allowing for increased interaction and adsorption of hydrogen molecules. This confinement effect can result in a significant increase in hydrogen density compared to bulk conditions. Due to limitations and difficulties associated with experimental investigations of confined hydrogen, molecular dynamics (MD) simulations serve as a valuable tool to explore and obtain crucial properties such as thermal conductivity and other related characteristics. In the previous study, Rodrigo *et al* [10] successfully conducted computational studies using MD simulations to investigate thermodynamic and transport properties for the supercritical bulk hydrogen, employing the Mie potential. Their obtained results are found to be in agreement with the data provided by the National Institute of Standards and Technology (NIST).

In this study, we employ equilibrium molecular dynamics (EMD) simulations to investigate the thermal conductivity of hydrogen confined between two graphene [19], sheets. Our primary focus is to explore the factors that influence heat transfer in this confined system, including the number of H_2 molecules, temperature, and the height of the nanochannel. Additionally, we analyze the density profile to examine the adsorption of H_2 molecules along the walls of the nanochannel. Moreover, we obtain the phonon density of states (DOS) to gain fundamental insights and facilitate further discussion. Through these analyses, we aim to enhance our understanding of the thermal properties of confined hydrogen and provide valuable insights for potential applications in nanoscale heat transfer and energy storage.

Computational method

Using EMD, we implement a series of simulations to calculate thermal conductivity of confined hydrogen molecules between two graphene sheets. All simulations were done through LAMMPS package [20], as a classical molecular dynamics code.

Figure 1 illustrates the simulated nanochannel contained H_2 particles, depicting two graphene sheets as walls, positioned at the top and bottom. The Packmol software [21], was employed to generate initial configuration. The distance between walls (height) can be different in various simulations. The graphene sheet has dimensions of 32 Å × 34 Å. Periodic boundary conditions were applied to all directions. The box dimension in the z-direction is sufficiently large to prevent any interaction between the H_2 particles and their images in that direction (see figure 1).

Each H_2 molecules modeled as an uncharged single-site particle. Therefore, we ignore the details of molecule structure such as bond and charge. To describe interaction between H_2 particles, we used Mie potential which is a more general formulation of Lennard-Jones potential:

$$U_{Mie}(r_{ij}) = C\varepsilon_{ij}\left[\left(\frac{\sigma_{ij}}{r_{ij}}\right)^{\lambda_r} - \left(\frac{\sigma_{ij}}{r_{ij}}\right)^{\lambda_a}\right] \quad (1)$$

Table 1. The Mie parameters for H_2 molecule [10].

λ_r	λ_a	$(\varepsilon_{H-H}/k_B)K$	σ_{H-H}/Å
7.813	6	18.355	3.1586

where C is a constant defined as:

$$C = \frac{\lambda_r}{\lambda_r - \lambda_a}\left(\frac{\lambda_r}{\lambda_a}\right)^{\frac{\lambda_a}{\lambda_a-\lambda_r}} \tag{2}$$

where λ_r and λ_a are the repulsive and attractive exponent, respectively. In this potential, it is assume that the H_2 acts as a particle. The force field parameters can be found in table 1.

The radius cut-off for interaction between hydrogen molecules was considered as 4 σ_{H-H}. On the other hand, we assumed $\varepsilon_{C-H} = 0.00246$ eV and $\sigma_{C-H} = 1.975$ Å for the interaction between carbon atoms and hydrogen molecules. To obtain the mentioned coefficients, we assumed the Lennard-Jones coefficients of C atoms in graphene is equal to the carbon atom in phenyl alanine ring in the CHARMM force field. There is a carbon atom in phenyl alanine ring that bonded to three other carbon same as carbon atom in graphene. Also, for hydrogen atoms, we considered coefficient from TIP3P water model [22, 23]. After that we used Lorentz–Berthelot combination rule. Also, we do not define any interaction between carbon atoms in graphene and keep them fixed during simulation time. The decision to keep the graphene layers fixed was made as an approximation for the sake of computational efficiency and simplicity. However, it's important to acknowledge that this approximation may have implications on the accuracy of the model, particularly in capturing dynamic interactions and structural changes that could occur in real-world scenarios. The timestep was set 1 fs to integrate the equation of motion using the velocity Verlet algorithm. To keep temperature constant, the Nose–Hoover thermostat [24], was utilized with damping factor of 100 fs.

At first, to minimize energy of the system and prevent unphysical behavior, we used conjugate gradient method, a widely utilized optimization technique in computational physics. The minimizers bound the distance atoms may move in one iteration, so that you can relax systems with highly overlapped atoms (large energies and forces) by pushing the atoms off of each other.

After performing energy minimization, to achieve thermodynamic equilibrium, the system was coupled to the NVT ensemble for 5 ns of simulation time. During this period, the thermodynamic quantities reached their final values and started fluctuating around the average them. Following the equilibration stage, we proceeded to the production stage where data was collected from the simulation. The production stage involved running the simulation for another 5 ns.

In the production stage, we used Green–Kubo method [25–27], to calculate the in-plane thermal conductivity which is the average thermal conductivity in x and y directions. The Green–Kubo formulas relate the ensemble average of the auto-correlation of the heat flux (represented by $\langle \ldots \rangle$) to the thermal conductivity:

$$\kappa_{xy} = \frac{V}{2k_B T^2}\int_0^\infty [\langle J_x(0)J_x(t)\rangle + \langle J_y(0)J_y(t)\rangle]\,\mathrm{d}t \tag{3}$$

where V, J_x, and J_y are the volume, heat flux in x and y-directions, respectively. The heat flux vector can be obtained through equation below:

$$\boldsymbol{J} = \frac{1}{V}\left[\sum_i e_i \mathbf{v}_i - \sum_i \mathbf{S}_i \mathbf{v}_i\right] \tag{4}$$

where e_i in the first term of the equation is the per-atom energy (potential and kinetic) and $\mathbf{S}_i$ in the second term is the per-atom stress tensor. Also, $\mathbf{v}_i$ denotes the velocity of atom i. Furthermore, the summations run over all particles.

Moreover, to explore the phonon DOS, we calculate the Fourier transformation of the velocity auto-correlation using the equation below:

$$P(\omega) = \frac{m}{k_B T}\int_0^\infty \mathrm{e}^{-\mathrm{i}\omega t}\langle \mathbf{v}(0).\mathbf{v}(t)\rangle\,\mathrm{d}t \tag{5}$$

Where the m, $\mathbf{v}$, and ω are the H_2 molecule, velocity, and the phonon angular frequency.

Fundamentally, molecular hydrogen should be approached from a quantum mechanics perspective. Nonetheless, it is feasible to employ a classical treatment under certain circumstances, as long as two specific conditions are fulfilled [28]. The first condition related to the de Broglie thermal wavelength:

$$\Lambda = \left(\frac{h^2}{2\pi m k_B T}\right)^{1/2} \tag{6}$$

where Λ is the de Broglie thermal wavelength and h is the Plank's constant. The m, k_B, and T are the hydrogen mass, Boltzmann constant, and absolute temperature, respectively. To suppose the system as a classical system, the de Broglie thermal wavelength should be less than the mean nearest distance between hydrogen molecules, which can be specified by $a = \left(\frac{V}{N}\right)^{1/3}$, where V and N are the system volume and the number of the hydrogen molecules. In the worst case, we have $\Lambda = 0.87$ Å at $T = 200$ K and also $a = 3.31$ Å at $N = 150$ and effective height of nanochannel 5 Å, therefore $\Lambda \ll a$. Hence, based on this criterion, we can neglect the quantum effect and use the classical approach. When temperature rises and number of H_2 decreases, then the quantum effect diminishes.

Rotational temperature is another condition that must be satisfied in order for the system to be considered classical:

$$\Theta_{\mathrm{rot}} = \frac{h^2}{8\pi^2 I k_B} \tag{7}$$

where Θ_{rot} and I are the rotational temperature and the moment of inertia, respectively. In order for a classical hypothesis to hold true, the rotational temperature should be lower than the absolute temperature being considered. In the case of molecular hydrogen, it is $\Theta_{\mathrm{rot}} = 86$ K. We implement simulations for temperatures exceeding 200 K. It should be noted that in instances where a system exhibits classical

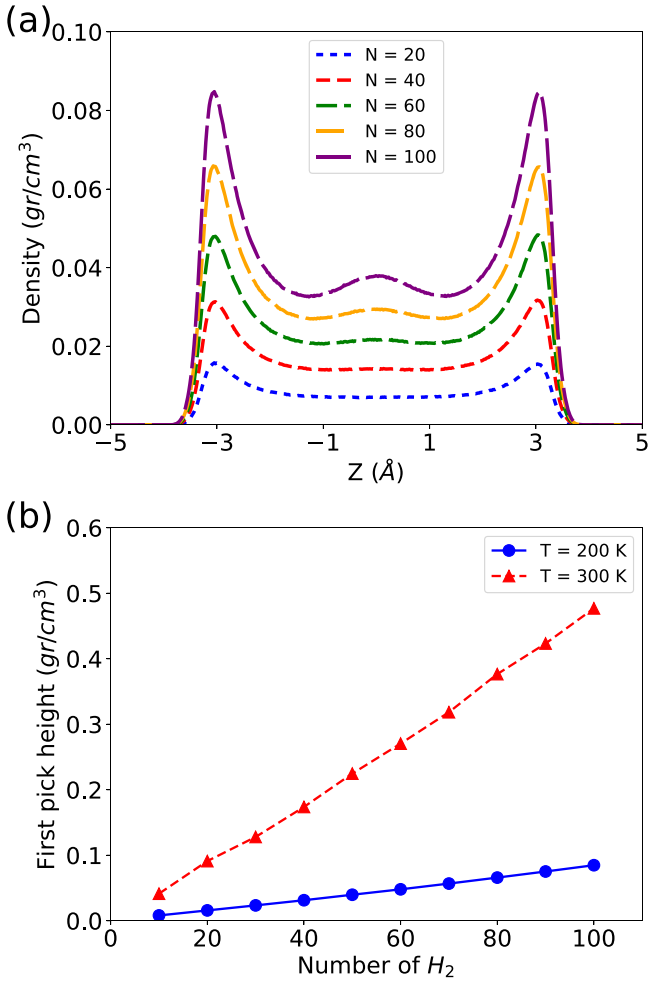

Figure 2. (a) The variation of local mass density of nano-confined hydrogen versus Z for five different number of H_2 molecules. Temperature is 200 K and the height of nanochannel is $h = 10$ Å. (b) the height of the first peak in the density profile plotted against the number of H_2 molecules exhibits a clear linear trend.

behavior, the influence of quantum effects tends to diminish. By treating the system classically, we simplify the computational model and enhance efficiency, but the results may exhibit slight deviation. This variance is evident in [10], where our employed model is based on the findings of that particular paper. The employed model successfully describes the thermophysical properties of H_2.

Results and discussion

Using EMD, the thermal conductivity was studied for the different configurations. When hydrogen molecules was placed inside nanochannel, the molecules adsorb on the walls that leads to an increase in the density of hydrogen near the wall.

To represent that, at first, we divided the system along the Z direction with bin size of 0.02 Å and calculated the mass density at each bin and averaged over 500 ps, utilizing each step in averaging process. As depicted in figure 2(a), the

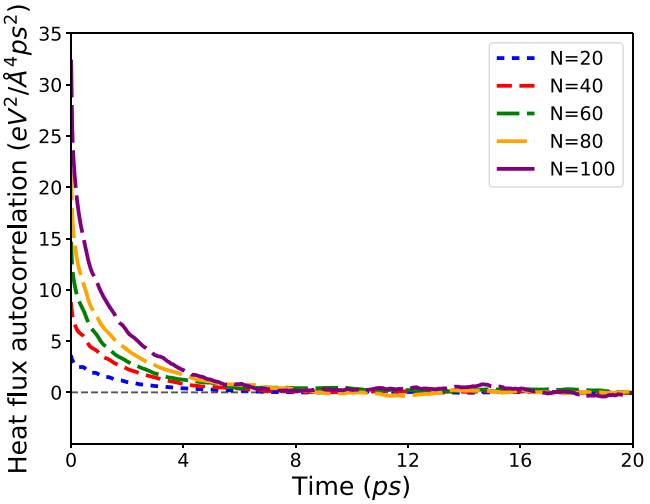

Figure 3. Heat flux auto-correlation in x direction versus time. In the plot $h = 10$ Å, and $T = 200$ K.

density profiles were plotted for temperature of 200 K and the height of nanochannel 10 Å.

As seen from the density profile, it is evident that H_2 molecules adsorb on the wall at a distance equal to σ_{C-H} approximately. When the number of molecules increases, the density of the molecules at the center of nanochannel $Z = 5$ Å increases and create a dense layer at that position. Furthermore, the density behavior near the wall holds significant interest as it relates to the thermal conductivity characteristics. To investigate this correlation, we examined the first peak in the density profile as a function of the number of H_2 molecules. In figure 2(b), we observe that the density near the wall increases with the rising number of H_2 molecules, and this trend holds true for two different temperatures. Notably, the slope of the curve is lower for $T = 200$ K compared to $T = 300$ K.

The heat flux auto-correlation was determined by assuming a correlation length of 20 ps. Within this specified length, the correlation of the heat flux approaches zero and diminishes. Figure 3 illustrates a gradual decrease of the heat flux auto-correlation until it reaches zero and fluctuate around it.

Subsequently, we proceeded to compute the in-plane thermal conductivity using equation (3). This involved conducting a series of five simulations with varying initial conditions, achieved by altering the random velocity at the beginning of each simulation. Here the reported values of thermal conductivity represent the average outcome obtained from these five simulations. Also the error bars calculated via standard deviation from five results.

As seen in figure 4 the thermal conductivity increases linearly with increasing number of H_2 molecules. This behavior was also seen in the bulk hydrogen according the NIST data [29, 30] (see table 2). According to the information provided by NIST, as the pressure increases, which corresponds to an increase in the number of molecules, the thermal conductivity also increases linearly in the range that we studied. The thermal conductivity in a nano-confined with 100 H_2 molecules is 12 times greater than that of the bulk

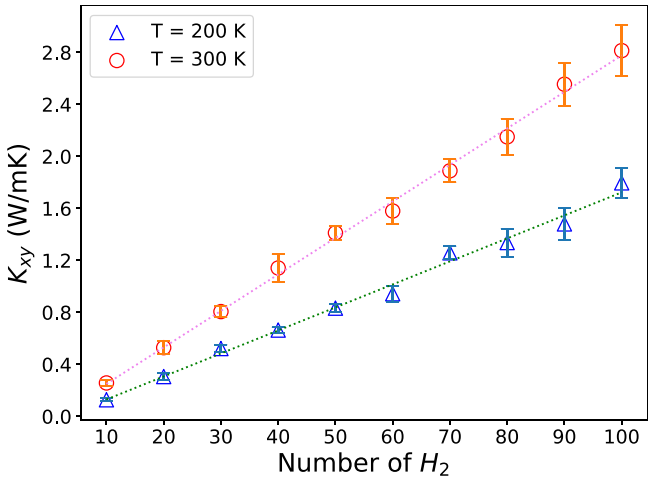

Figure 4. In-plane thermal conductivity versus the number of H_2 molecules. The height is 10 Å.

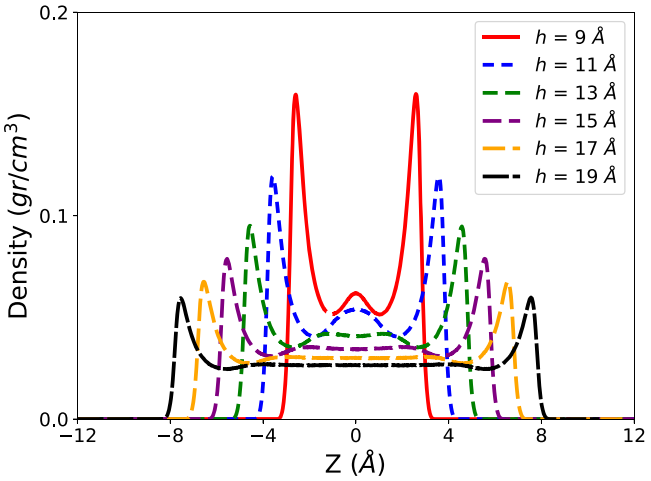

Figure 6. Density profile in Z direction for various height of nanochannel (h). The temperature and number of H_2 molecules are 200 K and 150, respectively.

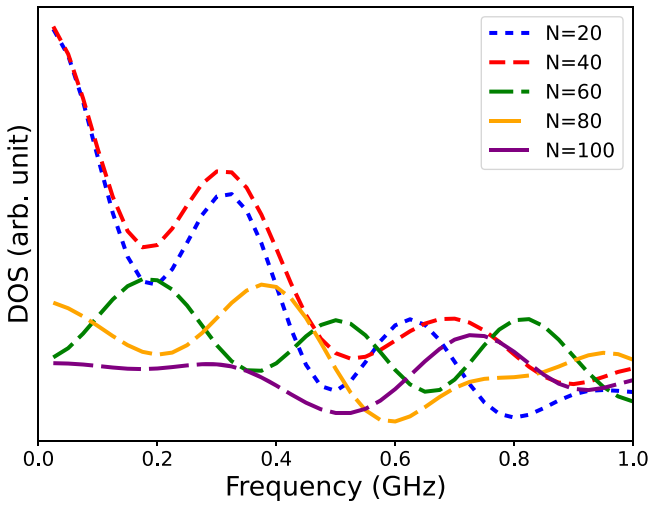

Figure 5. Phonon density of states for five setup with different number of H_2 molecules. The temperature and the height of nanochannel are 200 K and 10 Å, respectively.

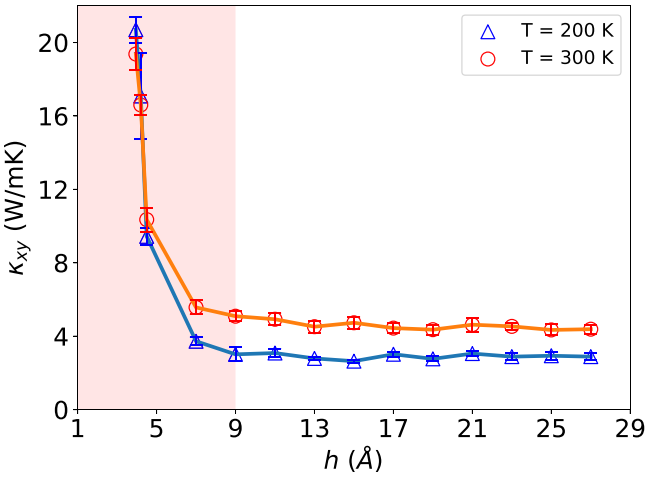

Figure 7. Thermal conductivity of confined H_2 molecules versus Height of nanochannel. The temperature is 200 K and the number of H_2 molecules is 150. For comparison, the thermal conductivity of bulk hydrogen stands at approximately 0.18 W mK^{-1} [29, 30] under conditions of $T = 200$ K and a density of 0.035 gr ml^{-1}, corresponding to a confined system with height of 8 Å.

Table 2 A comparison of thermal conductivity between our results and NIST data [29, 30]. As the number of H_2 rises, the confinement impact becomes increasingly evident.

Number of H_2	Pressure (bar)	Our results (W/mK) (nano-confined)	NIST data (W/mK) (bulk)
10	8	0.128	0.1342
20	17.96	0.307	0.1357
30	27.41	0.522	0.1370
40	39.02	0.664	0.1385
50	50.21	0.833	0.1398
60	63.2	0.944	0.1412
70	78.3	1.259	0.1427
80	93.06	1.338	0.1443
90	112.06	1.481	0.1462
100	129.16	1.797	0.1479

material. The molecules have been absorbed by the wall, causing them to attain a higher level of order. As a result, this increased order has led to a higher thermal conductivity compared to the gas. Furthermore, we observe a consistent trend between the thermal conductivity and the first peak density in the density profile (figure 2(b)). This suggests that the density near the wall plays a crucial role in determining the behavior of thermal conductivity.

Furthermore, we expected an increasing behavior because when the number of H_2 molecules increases, the gas molecules become more closely packed together. This higher molecular density leads to more frequent collisions between molecules, resulting in a more efficient transfer of thermal energy. The increased number of molecular collisions allows heat to be transferred more rapidly through the gas, leading to

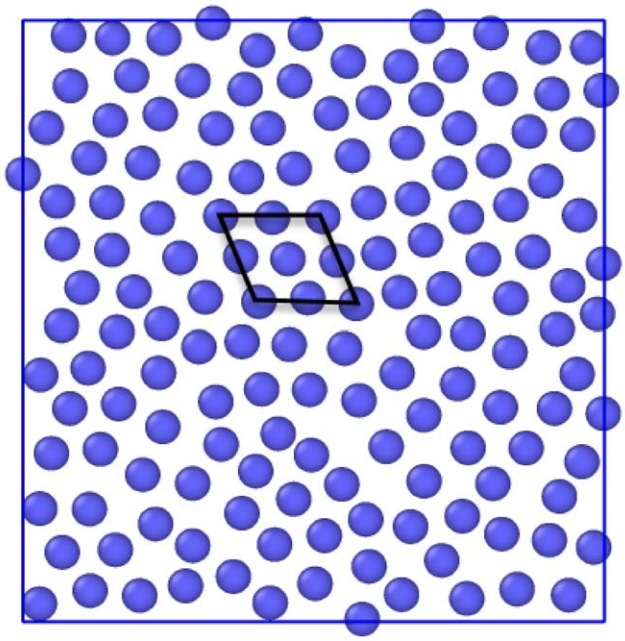

Figure 8. The top view snapshot of the H_2 molecules at a height of nanochannel 4 Å reveals a relative degree of ordering at a local level. The walls have been omitted in the visualization for clarity. The temperature is set at 200 K, and there are 150 H_2 molecules in the system.

an increase in thermal conductivity. Moreover, intermolecular interactions become more significant. The closer proximity of molecules due to increased density leads to stronger intermolecular interactions. These interactions facilitate the transfer of thermal energy through the gas, further enhancing the thermal conductivity.

In figure 5, the phonon DOS was calculated using equation (5) and plotted against the number of H_2 molecules. It is evident that the DOS varies among systems with different numbers of molecules. This discrepancy shows that the energy carrier modes differ from one system to another, thereby causing variations in thermal conductivity.

Now, we aim to investigate the impact of the nanochannel height on the thermal conductivity. To achieve this, we vary the height of the nanochannel in the range of 3.95–27 Å and calculate the corresponding thermal conductivity values. The density profile were plotted in figure 6. In the profile, it again was observed that in all heights the H_2 molecules adsorb on the wall, but when the height increases the density decreases near the wall. Similar density profiles have been observed in confined water [2]. In wide nanochannels, there is a uniform density at the center of the nanochannels, in contrast to systems studied at low temperatures or high pressures, where a layered density pattern is observed. In the case of narrow nanochannels, an additional layer is observed due to the higher pressure, as the number of H_2 molecules remains constant.

The dependence of thermal conductivity on the height of nanochannels is highly intriguing, particularly when the number of H_2 molecules remains constant. Therefore, we conducted a series of simulation to explore the effect of height in the mentioned range with 150 H_2 molecules. As depicted in

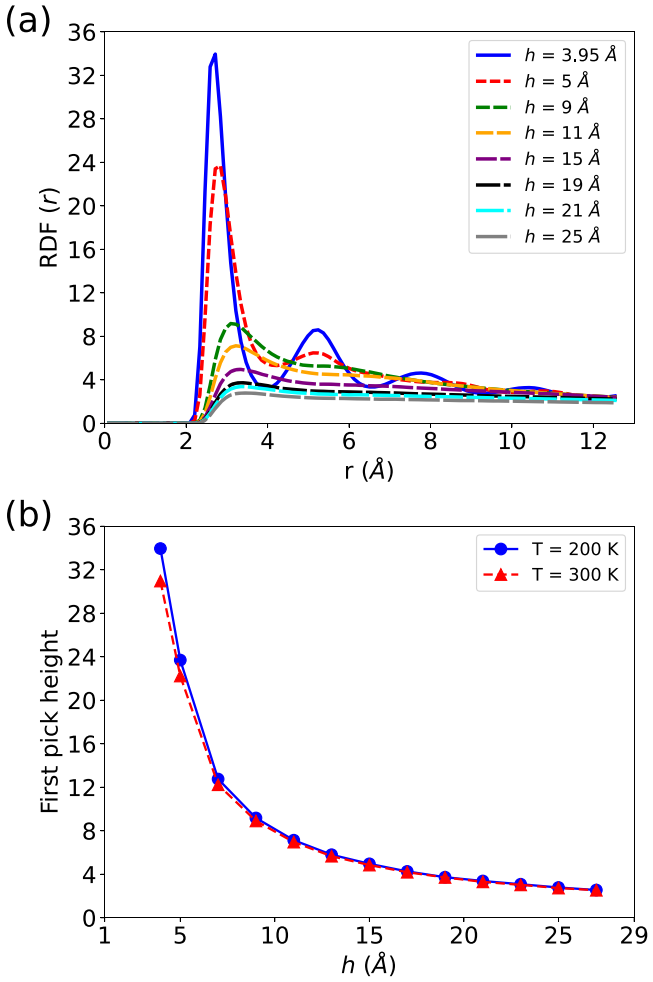

Figure 9. (a) The radial distribution function for two nanochannel heights. The temperature is 200 K and number of H_2 molecules is 150 and (b) the first pick height versus height of nanochannel. An observable correlation exists between the height of the first peak in the radial distribution function and the thermal conductivity, as depicted in figure 7.

figure 7. The thermal conductivity decreases via increasing the height of nanochannels. Two regions in the thermal conductivity exhibit significance. The first region, marked in pink, corresponds to $h \leqslant 9$ Å. Within this region, the thermal conductivity shows notable sensitivity to the nanochannel height, with values ranging from approximately 3–21 $W\,mK^{-1}$ as the nanochannel height decreases from 9 to 4 Å. On the other hand, in the right region, the thermal conductivity shows no dependency on the nanochannel height. Within this region, the thermal conductivity remains approximately $\sim 3\,W\,mK^{-1}$. However, it is noteworthy that the thermal conductivity is significantly higher compared to the bulk system, primarily due to the presence of two walls. These walls have also a noticeable impact on the structural properties of the confined system.

Interestingly, it was observed that within left regime, the H_2 molecules exhibit a relative degree of ordering at a local level (see figure 8). Degree of ordering can be seen by comparing the radial distribution function for two nanochannel heights in figure 9(a). As depicted in figure 9(a), at

lower nanochannel heights, hydrogen exists in a liquid phase, whereas for larger nanochannel heights, hydrogen transitions into a gaseous phase.

Similar to the first peak density in the density profile, we can also explore the first peak in the radial distribution function concerning the nanochannel height. Figure 9(b) reveals that the curve's behavior closely resembles that of the thermal conductivity. This strong correlation between the first peak density and the thermal conductivity highlights their interdependence and importance in characterizing the system.

Conclusion

Using EMD, we studied the thermal conductivity of the confined H_2 molecules between two graphene walls. Firstly, it was observed that as the number of H_2 molecules increased, the thermal conductivity showed a linear increase. This behavior is consistent with the data reported for bulk hydrogen and can be attributed to the increased molecular density, leading to more frequent collisions and stronger intermolecular interactions. The absorption of molecules by the nanochannel walls further enhanced the thermal conductivity by promoting a higher level of molecular order and facilitating efficient heat transfer. Furthermore, an exploration of the impact of nanochannel height on thermal conductivity revealed intriguing results. The density profiles demonstrated that the H_2 molecules adsorb on the walls regardless of the height, but the density near the wall decreases as the height increases. Notably, the thermal conductivity exhibited a decreasing trend with increasing height, emphasizing the significance of factors such as molecular ordering and density distribution in influencing heat transfer behavior. Within the explored height range, two distinct regions were identified in the thermal conductivity plot. In the first region, where the $h \leqslant 9$ Å, the thermal conductivity displayed notable sensitivity to the nanochannel height. In contrast, the thermal conductivity remained approximately constant ($\sim 3\ \mathrm{W\,mK^{-1}}$) in the right region. Nonetheless, the presence of two walls in the confined system significantly elevated the thermal conductivity compared to the bulk system. We have also discovered a robust correlation between the thermal conductivity and the first peak in both the density profile and the radial distribution function. These findings suggest a strong relationship between these two key properties, shedding light on their interconnected nature.

Data availability statement

The data cannot be made publicly available upon publication because they are not available in a format that is sufficiently accessible or reusable by other researchers. The data that support the findings of this study are available upon reasonable request from the authors.

ORCID iDs

Farrokh Yousefi https://orcid.org/0000-0001-7427-5363
Omid Farzadian https://orcid.org/0000-0001-7741-5552

References

[1] Zhao Z, Sun C and Zhou R 2020 Thermal conductivity of confined-water in graphene nanochannels *Int. J. Heat Mass Transf.* **152** 119502
[2] Zhao Z, Jin Y, Zhou R, Sun C and Huang X 2023 Unexpected behavior in thermal conductivity of confined monolayer water *J. Phys. Chem.* **127** 4090–8
[3] Jalali H, Lotfi E, Boya R and Neek-Amal M 2021 Abnormal dielectric constant of nanoconfined water between graphene layers in the presence of salt *J. Phys. Chem.*B **125** 1604–10
[4] Fumagalli L *et al* 2018 Anomalously low dielectric constant of confined water *Science* **360** 1339–42
[5] Hamid I, Jalali H, Peeters F M and Neek-Amal M 2021 Abnormal in-plane permittivity and ferroelectricity of confined water: from sub-nanometer channels to bulk *J. Chem. Phys.* **154** 114503
[6] Shekarforoush S, Jalali H, Yagmurcukardes M, Milošević M V and Neek-Amal M 2020 Optoelectronic properties of confined water in angstrom-scale slits *Phys. Rev.* **102** 235406
[7] Joseph S and Aluru N R 2008 Why are carbon nanotubes fast transporters of water? *Nano Lett.* **8** 452–8
[8] Ghosh K and Krishnamurthy C V 2018 Structural behavior of supercritical fluids under confinement *Phys. Rev.*E **97** 012131
[9] Jabbari F, Rajabpour A and Saedodin S 2017 Thermal conductivity and viscosity of nanofluids: a review of recent molecular dynamics studies *Chem. Eng. Sci.* **174** 67–81
[10] Bartolomeu R A C and Franco L F M 2020 Thermophysical properties of supercritical H_2 from molecular dynamics simulations *Int. J. Hydrog. Energy* **45** 16372–80
[11] van Rooijen W A, Habibi P, Xu K, Dey P, Vlugt T J H, Hajibeygi H and Moultos O A 2023 Interfacial tensions, solubilities, and transport properties of the $H_2/H_2O/NaCl$ system: a molecular simulation study *J. Chem. Eng. Data* **69** 307–19
[12] Johnston B, Mayo M C and Khare A 2005 Hydrogen: the energy source for the 21st century *Technovation* **25** 569–85
[13] Mahlia T M I, Saktisahdan T J, Jannifar A, Hasan M H and Matseelar H S C 2014 A review of available methods and development on energy storage; technology update *Renew. Sustain. Energy Rev.* **33** 532–45
[14] Kovač A, Paranos M and Marciuš D 2021 Hydrogen in energy transition: a review *Int. J. Hydrog. Energy* **46** 10016–35
[15] Zivar D, Kumar S and Foroozesh J 2021 Underground hydrogen storage: a comprehensive review *Int. J. Hydrog. Energy* **46** 23436–62
[16] Tarkowski R 2019 Underground hydrogen storage: characteristics and prospects *Renew. Sustain. Energy Rev.* **105** 86–94
[17] Bouwman P 2014 Electrochemical hydrogen compression (EHC) solutions for hydrogen infrastructure *Fuel Cells Bull.* **2014** 12–6
[18] Nordio M, Rizzi F, Manzolini G, Mulder M, Raymakers L, Van Sint Annaland M and Gallucci F 2019 Experimental and modelling study of an electrochemical hydrogen compressor *Chem. Eng. J.* **369** 432–42
[19] Geim A K and Novoselov K S 2007 The rise of graphene *Nat. Mater.* **6** 183–91

[20] Plimpton S 1995 Fast parallel algorithms for short-range molecular dynamics *J. Comput. Phys.* **117** 1–19
[21] Martínez L, Andrade R, Birgin E G and Martínez J M 2009 PACKMOL: A package for building initial configurations for molecular dynamics simulations *J. Comput. Chem.* **30** 2157–64
[22] Best R B, Zhu X, Shim J, Lopes P E M, Mittal J, Feig M and MacKerell A D 2012 Optimization of the additive CHARMM all-atom protein force field targeting improved sampling of the backbone ϕ, ψ and side-Chain χ_1 and χ_2 dihedral angles *J. Chem. Theory Comput.* **8** 3257–73
[23] Yousefi F, Farzadian O and Shafiee M 2023 Exploring the viscosity and structural behavior of confined hydrogen: a molecular dynamics approach *J. Mol. Liq.* **390** 123028
[24] Melchionna S, Ciccotti G and Lee Holian B 1993 Hoover NPT dynamics for systems varying in shape and size *Mol. Phys.* **78** 533–44
[25] Ramazani A, Reihani A, Soleimani A, Larson R and Sundararaghavan V 2017 Molecular dynamics study of phonon transport in graphyne nanotubes *Carbon* **123** 635–44
[26] Green M S 1954 Markoff random processes and the statistical mechanics of time-dependent phenomena: II. Irreversible processes in fluids *J. Chem. Phys.* **22** 398–413
[27] Kubo R 1966 The fluctuation-dissipation theorem *Rep. Prog. Phys.* **29** 306
[28] Jean-Pierre H and McDonald I R 2013 *Theory of Simple Liquids: with Applications to Soft Matter* (Academic press)
[29] Assael M J, Assael J-A M, Huber M L, Perkins R A and Takata Y 2011 Correlation of the thermal conductivity of normal and parahydrogen from the triple point to 1000 K and up to 10 Mpa *J. Phys. Chem. Ref. Data* **40** 033101
[30] Anon 2023 2023 NIST Standard Reference Database Number 69